Boosting biomethane yield and production rate with graphene: the potential of direct interspecies electron transfer in anaerobic digestion

Richen Lin, Jun Cheng, Jiabei Zhang, Junhu Zhou, Kefa Cen, Jerry D. Murphy

PII: S0960-8524(17)30656-9
DOI: http://dx.doi.org/10.1016/j.biortech.2017.05.017
Reference: BITE 18043

To appear in: *Bioresource Technology*

Received Date: 13 March 2017
Revised Date: 30 April 2017
Accepted Date: 3 May 2017

Please cite this article as: Lin, R., Cheng, J., Zhang, J., Zhou, J., Cen, K., Murphy, J.D., Boosting biomethane yield and production rate with graphene: the potential of direct interspecies electron transfer in anaerobic digestion, *Bioresource Technology* (2017), doi: http://dx.doi.org/10.1016/j.biortech.2017.05.017

Boosting biomethane yield and production rate with graphene: the potential of direct interspecies electron transfer in anaerobic digestion

Richen Lin[a,b,c], Jun Cheng[a,*], Jiabei Zhang[a], Junhu Zhou[a], Kefa Cen[a], Jerry D. Murphy[b,c]

[a] *State Key Laboratory of Clean Energy Utilization, Zhejiang University, Hangzhou 310027, China*

[b] *MaREI Centre, Environmental Research Institute, University College Cork, Cork, Ireland*

[c] *School of Engineering, University College Cork, Cork, Ireland*

Abstract

Interspecies electron transfer between bacteria and archaea plays a vital role in enhancing energy efficiency of anaerobic digestion (AD). Conductive carbon materials (i.e. graphene nanomaterial and activated charcoal) were assessed to enhance AD of ethanol (a key intermediate product after acidogenesis of algae). The addition of graphene (1.0 g/L) resulted in the highest biomethane yield (695.0 ± 9.1 mL/g) and production rate (95.7 ± 7.6 mL/g/d), corresponding to an enhancement of 25.0% in biomethane yield and 19.5% in production rate. The ethanol degradation constant was accordingly improved by 29.1% in the presence of graphene. Microbial analyses revealed that electrogenic species of *Geobacter* and *Pseudomonas* along with archaea *Methanobacterium* and *Methanospirillum* might participate in direct interspecies electron transfer (DIET). Theoretical calculations provided evidence that graphene-based DIET can sustained a much higher electron transfer flux than conventional hydrogen transfer.

* Corresponding author: Prof. Dr. Jun Cheng, State Key Laboratory of Clean Energy Utilization, Zhejiang University, Hangzhou 310027, China. Tel.: +86 571 87952889; fax: +86 571 87951616. E-mail: juncheng@zju.edu.cn

Keywords: Graphene; activated charcoal; ethanol; direct interspecies electron transfer; anaerobic digestion.

1. Introduction

Anaerobic digestion (AD) of wet organic biomass for biogas production provides a sustainable route to reduce fossil fuel use and greenhouse gas emissions, whilst producing alternative dispatchable energy (Shen et al., 2015). The biogas industry developed rapidly in Europe, in particular in Germany with 62% of the total biogas plants (Torrijos, 2016). Biogas satisfied 4.7% of electricity and 1% of heat demand in Germany in 2014 (Torrijos, 2016). Due to the high growth rate and carbohydrate content, algae including micro- and macro-algae are considered to be a viable alternative energy feedstock that is devoid of the major drawbacks associated with first and second-generation feedstock (Chen et al., 2015; Nigam & Singh, 2011). However, AD of algae involving biological, chemical, and physical reactions can be limited by the long retention time, low biodegradation efficiency, and low biogas production rate. The energy conversion efficiency and process stability of AD can be easily disturbed by various biological and environmental factors, such as process temperature, pH value, hydrodynamics, and organic loading and detention time (Cheng & Call, 2016; Viggi et al., 2014).

The AD performance needs to be improved to make the process more economically viable. Optimizations of the process control variables were reported effective to minimize energy consumption and increase biogas production (Kusiak & Wei, 2012; Wei & Kusiak, 2012). Wei et al developed a data-driven prediction model to optimize biogas production from sludge, in which temperature, total solids, volatile solids and pH were employed as controllable variables. A 20.8%

increase was obtained when all controllable values were set to the optimal values (Wei & Kusiak, 2012). Many studies have focused on pretreatment development (such as thermal, mechanical, chemical and biological methods) to overcome feedstock recalcitrance and enhance subsequent AD performance (Ariunbaatar et al., 2014). The effects of various pretreatment methods are highly different depending on the feedstock characteristics. Nevertheless, pretreatment methods could be unsustainable in terms of environmental impacts, even if they enhance AD efficiency (Ariunbaatar et al., 2014; Carballa et al., 2011).

From a biological perspective, AD is carried out by different groups of microorganisms involved in hydrolysis, acidogenesis, acetogenesis and methanogenesis; interspecies electron transfer between syntrophic bacteria and methanogenic archaea plays a vital role in enhancing AD efficiency (Stams & Plugge, 2009). The predominant understanding for interspecies electron transfer in AD was based on mediated interspecies electron transfer (MIET) via hydrogen or formate (Rotaru et al., 2014b; Storck et al., 2016). MIET is normally endergonic under standard conditions and is feasible only at very low metabolite concentration (especially hydrogen) due to the thermodynamic constraints (Viggi et al., 2014). Recent findings revealed that direct interspecies electron transfer (DIET) via electrically conductive pili, mineral, or shuttle molecules is energetically more advantageous than MIET, because DIET does not require the multiple enzymatic steps to produce hydrogen as an electron carrier (Lovley, 2011; Zhao et al., 2015).

Conductive materials (such as nano-magnetite, graphite, biochar, activated carbon and carbon cloth) may avoid the energy consumption associated with the production of extracellular conductive pili and associated c-type cytochromes for the provision of biological electrical connections between cells (Kato et al., 2012; Liu et al., 2012; Zhao et al., 2015). Activated carbon

has been proven to promote DIET in AD of different types of substrates, such as ethanol, propionate, butyrate and glucose (Lee et al., 2016; Zhao et al., 2016b). The biomethane production rate in the presence of biochar increased by 16-25% in AD of propionate and butyrate (Zhao et al., 2016a). Carbon-based nanomaterials exhibited the potential to stimulate DIET using glucose and sucrose as substrates (Li et al., 2015; Tian et al., 2017). Tian et al. demonstrated that methanogenesis of glucose was improved by addition of graphene during long-term anaerobic digestion under low temperature (10-20 °C). Despite the establishment of DIET in pure and mixed cultures, the application of nano-scale carbonaceous materials in traditional AD requires further investigations to improve the AD performance.

As a highly-conductive nanomaterial, graphene has received heightened attention for biotechnological applications, such as electrode materials in microbial fuel cells (ElMekawy et al., 2016; Perreault et al., 2015). Graphene has known antimicrobial properties in some cases (Catherine et al., 2012; Nguyen et al., 2017), however, little is known about the impact of graphene on anaerobic microbial communities in AD. The unique physicochemical properties of graphene, notably its exceptionally high electric conductivity, large surface area and good mechanical strength, may provide a solution to improve the stability and efficiency of AD. Therefore, it is hypothesized that graphene can significantly facilitate DIET and enhance AD efficiency. However, to the best of our knowledge, the research of DIET in AD of ethanol in the presence of graphene is rather sparse. Theoretical comparison of electron transfer flux between graphene-based DIET and MIET have not been calculated previously. The interactions between nanomaterial and microbes in AD have not been revealed. In this study, ethanol was used as feedstock to investigate DIET in AD, as ethanol is a key intermediate product after acidogenesis of

algae feedstock (accounting for 15.6%-34.2% of total energy production (Xia et al., 2015; Xia et al., 2016)). The innovation and objectives of this study are as follows: (1) Compare the kinetics of biomethane production with different additions of graphene and activated charcoal in AD of ethanol; (2) Identify the bacterial and archaeal communities responsible for graphene-based DIET in AD; (3) Calculate the maximum electron transfer flux of MIET and graphene-based DIET for the first time.

2. Materials and methods

2.1. Inoculum and materials

The inoculum was sourced from a laboratory digester mainly treating cellulose. Graphene and activated charcoal were both purchased from Shanghai Aladdin Bio-Chem Technology Co., Ltd, China. The size of activated charcoal was approximately 10-32 mesh (equivalent to 0.5-1.7 mm). The micro size of graphene was around 5~10 μm, and the thickness of graphene nanoplatelets was between 4-20 nm. More details on physic-chemical properties of graphene are available in http://www.aladdin-e.com/up_files/docs/G139804.pdf.

2.2. Experimental design

Batch experiments of AD were conducted in glass fermenters (300 mL working volume). Each bottle contained 2.5 mL of ethanol as feedstock and 250 mL of activated sludge as inoculum. The initial pH was adjusted to 7.5 ± 0.1 through use of 6 M HCl and 6 M NaOH solution. Subsequently different amounts of graphene and activated charcoal were separately added into the glass bottles. The concentrations of graphene were set as 0, 0.5, 1.0 and 2.0 g/L. Considering the

electric conductivity of activated charcoal is much lower than that of graphene, the concentrations of activated charcoal were set as 0, 5, 10, 20 and 30 g/L. Deionized water was added to adjust the total solution to 300 mL. Afterwards, all the bottles were sealed with rubber stoppers, purged with nitrogen gas for 10 min, and maintained at 35 ± 1.0 °C during AD. The produced biogas and liquid solution during methanogenesis were sampled and analyzed at an interval of 2 d. The pH value of solutions was readjusted to 7.5 every 2 d in order to prevent a severe pH drop during AD. All the experiments were conducted in duplicate.

2.3. Microbial community analysis

A volume of 5ml of anaerobic sludge was collected from the bottom of the reactors after the AD experiments. The sludge samples were rinsed with phosphate-buffered saline and then centrifuged for 10 min at 4 °C. The pretreated samples were stored at -20 °C until further use. The microbial community was characterized using high-throughput 16S rRNA pyrosequencing. DNA extraction was performed following the manufacturer's protocol (http://omegabiotek.com/store/wp-content/uploads/2013/04/D5625-Soil-DNA-Kit-101216-online-1.pdf). The DNA samples were amplified in two independent PCR reactions with primers spanning the V3-V4 hypervariable region of the 16S rRNA gene. PCR products were checked in 2% agarose gel to determine the success of amplification. Samples were pooled together in equal proportions based on their molecular weight and DNA concentrations. Then the samples were purified using calibrated Ampure XP beads. The pooled and purified PCR product was used to prepare the DNA library by following Illumina TruSeq DNA library preparation protocol. Sequencing was performed at MR DNA (www.mrdnalab.com, Shallowater, TX, USA) on a MiSeq

following the manufacturer's guidelines. Sequence data were processed using MR DNA analysis pipeline (MR DNA, Shallowater, TX, USA). Operational taxonomic units (OTUs) were defined by clustering at 3% divergence (97% similarity). Final OTUs were taxonomically classified using BLASTN against a curated database derived from GreenGenes, RDPII and NCBI (www.ncbi.nlm.nih.gov, http://rdp.cme.msu.edu) (DeSantis et al., 2006).

2.4. Microscope observation

The microbial morphology of sludge in response to graphene was observed on a field emission scanning electronic microscope (SEM, Hitachi SU 8010, Japan) (Cheng et al., 2013). The samples from the reactors were fixed with 2.5% (v/v) glutaraldehyde at 4 °C, washed followed by stepwise dehydration in a gradient series of ethanol solutions and then CO_2 critical point dried. Samples were finally coated with gold and observed by SEM.

2.5. Analytical methods

The concentrations of biomethane and carbon dioxide were analyzed on a gas chromatography system (GC; Agilent 7820A, USA) equipped with a thermal conductivity detector and a 5A column. The concentrations of ethanol and acetate were analyzed on another GC system equipped with a flame ionization detector and a DB-FFAP column (Lin et al., 2016).

Biomethane yield was simulated by the modified Gompertz equation (Eq. 1), and kinetic parameters (H_m, maximum methane yield potential, mL/g ethanol; R_m, peak methane production rate, mL/g ethanol/h; λ, lag-phase time of methane production, h; and T_m, peak time of methane fermentation, h) were calculated using Origin 8.5 software.

$$H = H_m \exp\left\{-\exp\left[\frac{R_m e}{H_m}(\lambda - t) + 1\right]\right\} \quad (1)$$

The degradation of ethanol was assumed to fit a first-order model (Eq. 2), where C_e is ethanol concentration (mM), C_{e0} is the initial ethanol concentration (mM), and k_e is the ethanol degradation rate constant (d^{-1}).

$$C_e = C_{e0} \exp(-k_e t) \quad (2)$$

The overall electron recovery after AD of ethanol was calculated according to Eq. 3.

$$\text{Electron revovery } \% = \frac{\text{Actual biomethane yield}}{\text{Stoichiometric conversion of ethanol to biomethane}} \times 100\% \quad (3)$$

3. Results and discussion

3.1 Effects of conductive materials on biomethane production kinetics in anaerobic digestion

To evaluate the effects of the conductive materials (graphene and activated charcoal) on the performance of AD, ethanol (a low-molecular substrate) was used as a model carbon source. The effects of graphene and activated charcoal on biomethane yield and production rate are shown in Fig. 1 a and b. The biomethane yield from ethanol without conductive material addition was 556.1±53.3 mL/g after 12 d. The peak biomethane production rate was obtained as 80.1±0.2 mL/g/d at 4 d. The addition of 20.0 g/L of activated charcoal gave a maximum biomethane yield of 627.2±30.7 mL/g. The peak biomethane production rate was obtained as 91.1±18.6 mL/g/d. The biomethane yield and peak biomethane production rate were greatly enhanced by 12.8% and 13.7%, respectively. The biomethane yields achieved with 5.0, 10.0 and 30.0 g/L of activated charcoal were lower than that with 20.0 g/L of activated charcoal (data were not shown in Fig. 1 in order to make it more explicit). Therefore, the optimal concentration of 20.0 g/L activated

charcoal was used for further comparison with different concentrations of graphene. It was proven that carbonaceous materials such as graphite, biochar, and carbon cloth are capable of promoting methane fermentation and chemical oxygen demand removal (Zhao et al., 2015). Li et al. reported that the electrical conductance of the sludge was enhanced in the presence of carbon nanotube, which might promote DIET among fermentative bacteria and methanogens in the AD process (Li et al., 2015). Thus, it is hypothesized that materials with higher conductivity may play a more significant role in promoting DIET. Fig. 1 shows that the biomethane yield positively increased from 556.1±53.3 (0 g/L graphene) to 670.9±16.0 (0.5 g/L graphene), 695.0±9.1 (1.0 g/L graphene) and 662.9±14.7 mL/g (2.0 g/L graphene). The optimal concentration of graphene (1.0 g/L) resulted in a 25.0% increase in biomethane yield and a 19.5% increase in peak biomethane production rate. However, on further increasing the graphene concentration to 2.0 g/L, the biomethane yield slightly decreased to 662.9±14.7 mL/g. This result was probably ascribed to the microbial inhibition effect by the high concentration of graphene, indicating that cytotoxicity could become a limiting factor when applying nanomaterials in AD. Cytotoxicity of carbon nanomaterials (such as graphene and carbon nanotube) to microbes has been demonstrated using different microbial strains such as *Escherichia coli* and *Bacillus subtilis* (Liu et al., 2011; Pasquini et al., 2012; Zhu et al., 2014). The toxicological molecular mechanisms of nanomaterials remained limited, but a possible explanation was related to the synergistic impacts of cell membrane perturbation and oxidative stress (Qu et al., 2015).

It was noted that the optimal graphene addition resulted in a more significant enhancement of biomethane production as compared to the optimal activated charcoal addition (even with a concentration of 20.0 g/L). This result can be ascribed to the following reasons: (1) The electrical

conductivity of graphene is much higher than that of activated charcoal, resulting in higher electron transfer efficiency in DIET; (2) The micro size of graphene is much smaller, resulting in a higher specific surface area and a better interaction with microbes.

The kinetic parameters of biomethane production fitted by the modified Gompertz equation are shown in Table 1. The kinetics of biomethane production were evaluated in terms of the biomethane yield potential (H_m), peak biomethane production rate (R_m), lag phase time (λ) and peak time (T_m). The maximum biomethane yield potential (H_m, 718.4 mL/g) was achieved in the presence of 1.0 g/L graphene, corresponding to a value of 23.4% higher than the control. Accordingly, the peak biomethane production rate (R_m, 116.2 mL/g/h) was obtained with the addition of 1.0 g/L graphene, corresponding to a value of 33.7% higher than the control. The lag phase time (λ) and peak time (T_m) both reduced to a great extent in the presence of graphene. On comparison to graphene, the biomethane production performance in terms of biomethane yield potential and peak biomethane production rate was less enhanced with addition of activated charcoal, even at a high concentration of 20.0 g/L.

3.2 Effects of conductive materials on ethanol degradation in anaerobic digestion

The complete conversion of ethanol to biomethane in AD requires the combined acetogenic bacteria and methanogenic archaea mediating the three step reactions (Table 2). Acetogenic bacteria are responsible for converting ethanol into acetate and releasing electrons. Methanogenic archaea are responsible for converting produced acetate, carbon dioxide and electron into biomethane. The effects of graphene and activated charcoal on degradation of ethanol are shown in Fig. 2a. It was observed that ethanol was continuously consumed by acetogenic bacteria during

12 d of AD. Ethanol degradation was more rapid with the addition of conductive materials. In the presence of 1.0 g/L graphene and 20.0 g/L activated charcoal, 50.3% and 43.5% of ethanol were consumed in the first 2d of AD. Comparatively, only 32.0% of ethanol was consumed in the absence of conductive materials. Apparently, graphene played a significant role in rapid degradation of ethanol, which is possibly due to the high electrical conductivity and specific surface area. The ethanol degradation rate constants derived from the first-order equation are shown in Fig. 2b. In the absence of conductive materials, the calculated ethanol degradation rate constant was only 0.31±0.03 /d. This value increased to 0.37±0.04 /d and 0.40±0.03 /d with the addition of activated charcoal and graphene, respectively. The higher ethanol degradation rate constant indicated that the substrate degradation in AD can be significantly enhanced through the presence of conductive materials.

With continuous degradation of ethanol, acetate reached a peak concentration, and was subsequently depleted by aceticlastic methanogen (Fig. 2c). The highest acetate concentration of 58.1 mM was obtained at 6 d in the presence of 1.0 g/L graphene, as compared to acetate concentration of 43.4 mM in the absence of conductive materials. Ethanol and acetate were completely consumed at the end of AD (12 d). It was clearly observed that acetate generation by acetogenic bacteria and subsequent consumption by aceticlastic methanogens were much faster in the presence of graphene, resulting in promoted methanogenesis and enhanced biomethane yield. These result indicated that conductive materials are capable of promoting syntrophic reactions between acetogenic bacteria and methanogenic archaea, which facilitates substrate degradation and utilization for enhanced methanogenesis.

To evaluate the overall efficiency of ethanol conversion in AD, the electron recovery was

calculated in terms of biomethane yield and stoichiometric conversion of ethanol to biomethane (Fig. 2d). Consistent with the biomethane yield, the highest electron recovery of 95.1±1.2% was achieved in the presence of graphene, as compared to 76.1±7.3% in control group. The enhanced electron recovery was attributed to enhanced DIET efficiency with graphene. It was noteworthy that 100% conversion of ethanol to biomethane was almost impossible. This was mainly because the biodegradation of ethanol in AD not only generates acetate (Table 2) but also minor amounts of propionate, butyrate, or caproate along with the consumption of hydrogen. In addition, some energy derived from ethanol degradation is required to support microbial growth.

3.3 Microbial community analyses after anaerobic digestion

3.3.1. Bacterial community composition

The enhanced biomethane production was highly dependent on the syntrophic activities of electron-producing acetogens and electron-consuming methanogens. The changes in the microbial community might provide a clue to the reason for enhanced biomethane production. Bacterial and archaeal community structures at genus level after AD of ethanol are shown in Table 3 and 4. The taxonomic compositions of the initial inoculum were distinctly different from those fed with ethanol after AD. This result is ascribed to the assimilation effect as ethanol is the only carbon source, which selectively enriched strains favoring ethanol utilization.

In the original inoculum, *Clostridium* (10.1%), *Levilinea* (7.6%), and *Aminobacterium* (4.0%) were the three major bacterial genera. *Clostridium* are metabolically versatile(Lee et al., 2007) and are the predominant strains involved in dark hydrogen fermentation converting carbohydrates to hydrogen along with the production of volatile fatty acids (VFAs, such as acetate and butyrate).

Levilinea are recognized as an anaerobic fermentative bacterium, which ferment sugars and amino acids into hydrogen, acetic and lactic acids.(Yamada et al., 2006) *Aminobacterium* are capable of degrading amino acids to VFAs (Baena et al., 1998).

After the AD of ethanol without graphene, the dominant bacterial groups shifted to *Levilinea* (11.6%), *Clostridium* (8.6%), and *Geobacter* (8.4%). The abundance of amino acid-degrading *Aminobacterium* decreased to 2.1%, which can be ascribed to the absence of amino acids during AD. *Geobacter* were enriched from 0.3% (in initial inoculum) to 8.4% with ethanol as substrate. A variety of *Geobacter* species (such as *G. metallireducens*, *G. pickeringii*, and *G. lovleyi*) has the ability to utilize ethanol as an electron donor to support their growth metabolism (Lovley et al., 2011).

With the addition of graphene in AD, the dominant bacterial groups shifted to *Geobacter* (9.9%), *Pseudomonas* (6.9%) and *Levilinea* (6.2%). The abundance of *Geobacter* increased to 9.9% in the presence of graphene, as compared to 8.4% without graphene. The high electrical conductivity of graphene may contribute to the shift during AD. Graphene enhances the electron transfer during ethanol degradation by *Geobacter*, which in turn facilitates the growth of *Geobacter*. *Geobacter* are well-known iron-respiring bacteria and are distributed widely in anaerobic environments; they are among the most effective microorganisms for harvesting electrical current from organic compounds (Lovley et al., 2011). It has been reported that *Geobacter* play a significant role in performing DIET either directly through extracellular pili or using additional conductive materials (Cheng & Call, 2016). DIET was first documented in co-culture of *Geobacter* species, where *Geobacter metallireducens* is capable of transferring electrons derived from ethanol to the partner *Geobacter sulfurreducens* via electrically conductive

pili (Summers et al., 2010). DIET was also recorded in anaerobic digesters where *Geobacter* transfer electrons to *Methanosaeta* (Rotaru et al., 2014b). DIET may yield more energy than conventional MIET because there is less energy loss associated with the formation of intermediates and the subsequent reactions needed to oxidize them (Lovley, 2011; Zhao et al., 2015). This could be one plausible explanation for the acceleration of methanogenesis in the presence of graphene. Therefore, it is concluded that the predominance of *Geobacter* population (9.9%) found in the presence of graphene is a potent support for DIET in AD of ethanol. It was also found the abundance of *Pseudomonas* was greatly increased to 6.9% in the presence of graphene, as compared to only 1.9% without graphene. *Pseudomonas* species are recognized as electrogenic bacteria responsible for converting VFAs to electric current in microbial fuel cells (Freguia et al., 2010). *Pseudomonas* are also capable of converting ethanol to acetate along with the production of electrons. However, it was reported that *Pseudomonas* are unable to effectively transfer electrons derived from central metabolism to the outside of the cell (Lovley, 2006). It was demonstrated that *Pseudomonas aeruginosa* yielded poorly conductive pili (Reguera et al., 2005), which cannot be used as conduit for extracellular electron transfer. The addition of graphene in AD could act as an alternative to conductive pili and an aid in electron transfer from *Pseudomonas* to the methanogenic partners during AD, contributing to the enhanced growth of *Pseudomonas*. As a result, since the electrogenic bacteria of *Geobacter* and *Pseudomonas* species were found greatly enriched with the addition of graphene, they are proposed to be responsible for DIET in AD of ethanol.

3.3.2. Archaeal community composition

The archaeal community structures at genus level with/without graphene addition after AD of ethanol are shown in Table 4. The majority of archaeal communities were mainly comprised of 4 archaeal genera. In the original inoculum, *Methanosaeta* were the most dominant species accounting for 86.1% of the total abundance, followed by *Methanolinea* (6.4%), *Methanobacterium* (2.7%) and *Methanospirillum* (1.1%). *Methanosaeta* are often abundant in anaerobic digesters and are mainly acetate-consuming methanogens which cleave acetate into CH_4 and CO_2 (Table 2). *Methanosaeta* are also capable of receiving electrons via DIET for CO_2 reduction into CH_4 (Rotaru et al., 2014b). *Methanolinea*, *Methanobacterium* and *Methanospirillum* are conventionally recognized as hydrogen-consuming methanogens, which convert CO_2 and H_2 into CH_4 (Table 2).

After AD of ethanol, the dominant archaeal groups were greatly changed due to the acclimatization effect by ethanol. With the addition of graphene in AD, the dominant archaeal groups shifted to *Methanosaeta* (39.8%), *Methanobacterium* (34.9%) and *Methanolinea* (9.8%). It was noted that the abundance of *Methanosaeta* decreased to 39.8% in the presence of graphene as compared to 50.1% without graphene, suggesting that the pathway of CH_4 production by acetate cleavage was weakened. The abundance of *Methanolinea* decreased from 20.2% to 9.8% with the addition of graphene. Comparatively, *Methanobacterium* became more predominant, increasing from 24.0% to 34.9%, while *Methanospirillum* were enriched from 2.2% to 7.8%. The shift of archaeal structures indicated the metabolic pathway was changed in AD in the presence of graphene. To date, *Methanosarcina* and *Methanosaeta* species are the only methanogens known to participate in DIET by directly receiving electrons to reduce CO_2 into CH_4 (Rotaru et al., 2014a; Rotaru et al., 2014b). However, in this study the enrichment of *Methanobacterium* and

Methanospirillum with the addition of graphene proposes a possibility that they may play an important role in performing DIET.

The communities of bacteria and archaea observed in the presence of graphene provided a clue for the reason of enhanced biomethane production and also provided a mechanistic explanation. Taken together, electrogenic bacteria of *Geobacter* and *Pseudomonas* species along with archaea *Methanobacterium* and *Methanospirillum* may participate in DIET in AD of ethanol, contributing to the enhanced AD performance.

3.4 Effects of conductive materials on microbial morphologies after anaerobic digestion

Microbial morphologies after AD with/without graphene addition are shown in Fig. S1 in the Supplementary material. Rod-shaped cells with different lengths of 1-4 μm are predominant in both samples with/without graphene addition. It appears that cells are attached together (Fig. S1 c and d), forming microbial aggregates after digestion in the presence of graphene. The direct contact of cells in aggregates may allow direct electron transfer during AD. It is also observed that there are extracellular "microbial nanowires" (~50 nm) formed on cell surfaces, exhibiting typical characteristic of electrogenic bacteria (such as *Geobacter*). However, it is unknown if these microbial structures are electrically conductive. It was reported that the aggregates in the anaerobic reactors treating brewery wastes exhibited a high and metal-like conductance (Morita et al., 2011; Shrestha et al., 2014). The conductive property of aggregates was ascribed to that *Geobacter* species, which produce electrically conductive pili with a high and metal-like conductance (Morita et al., 2011).

3.5 Theoretical analysis of graphene-based direct interspecies electron transfer and interspecies hydrogen transfer

Interspecies electron transfer in AD can rely on either DIET (between electron-producing acetogens and electron-producing methanogens) or MIET with hydrogen as electron carrier. The simplified electron transfer mechanisms for DIET and MIET are illustrated in Fig. 3. To quantitatively compare the electron transfer efficiencies of DIET and MIET, the theoretical maximum electron carrier fluxes were calculated based on Nernst equation and Fick's diffusion law (Mao et al., 2015; Viggi et al., 2014). The detailed parameters for calculations were provided in the Supplementary material.

The maximum electron flux for the graphene-based DIET was calculated as following. Assuming that the electrons are released from ethanol degradation through electron-donating reaction (Table 2, $CH_3CH_2OH + H_2O \rightarrow CH_3COO^- + 5H^+ + 4e^-$, $\Delta G^{0\prime}$= -149.64 kJ/mol), then the electrons are directly transferred to methanogens via graphene. Methanogens reduce CO_2 to CH_4 through electron-consuming reaction (Table 2, $4H^+ + 4e^- + 1/2CO_2 \rightarrow 1/2CH_4 + H_2O$, $\Delta G^{0\prime}$= 93.98 kJ/mol). The maximum driving force for electron transfer is given by the redox potential (ΔE) of the overall reaction ($CH_3CH_2OH + 1/2CO_2 \rightarrow 1/2CH_4 + CH_3COO^- + H^+$, $\Delta G^{0\prime}$= -55.67 kJ/mol), which was calculated as 0.136 V. The resulting maximum electron flux via graphene was determined as approximately 7×10^{-4} A (see calculations in Fig. S2 in the Supplementary material).

To estimate the maximum H_2 flux in MIET, the concentrations of reactants and products were set identical to those in DIET. Fick's law is used to compute the rate of H_2 diffusion from the

acetogen to the methanogen (Mao et al., 2015). The maximum driving force for H_2 diffusion depends on the highest H_2 concentration generated by acetogens and the lowest H_2 concentration reached by methanogens. The highest H_2 concentration was calculated in terms of the electron-donating reaction (Table 2, $CH_3CH_2OH + H_2O \rightarrow CH_3COO^- + H^+ + 2H_2$, corresponding to $\Delta G' = 0$), and the lowest H_2 concentration was calculated in terms of the electron-consuming reaction (Table 2, $2H_2 + 1/2CO_2 \rightarrow 1/2CH_4 + H_2O$, corresponding to $\Delta G' = 0$). The obtained highest and lowest H_2 concentrations were approximately 70.8 μM and 1.5 nM, respectively. Therefore, a maximum H_2 flux was achieved as approximately 3.6×10^{-6} nmol/s, theoretically corresponding to an equivalent electric current of 7×10^{-10} A (see calculations in Fig. S3 in the Supplementary material).

Clearly there is a huge difference in maximum electron transfer rate between graphene-based DIET and MIET via hydrogen. The maximum electron flux calculated in DIET is theoretically around 10^6 times higher than that obtained in MIET. The calculations also give a clue that activated charcoal may not be effective to conduct DIET due to its poor electrical conductivity (~5 orders of magnitude lower than graphene (Adinaveen et al., 2016). It should be pointed out that several assumptions were made to calculate the electron fluxes, such as the microbial cell shape, average distance between cells, graphene shape, no energy loss as heat during electron transfer, and no energy consumption for microbial growth. The driving force for electron transfer is assumed to be totally determined by Gibbs free energy ($\Delta G' = 0$), which does not consider the energy conserved for microorganism growth and energy loss as heat during electron transfer. However, a free energy of about -20 to -15 kJ/mol is normally required to support syntrophic microbial growth (Schink, 1997). These assumptions will undoubtedly result in the inaccuracy on

the final calculated value for MIET and DIET, which necessitate a more accurate model development. However, in spite of these considerations, the computed difference between MIET and DIET is so large that the kinetic advantage of the DIET via graphene is apparent. The result provides evidence that graphene-based DIET can intrinsically sustain electric current flux up to 6 orders of magnitude than that of hydrogen-based MIET, allowing for more efficient electron transfer in syntrophic mechanism in AD of ethanol.

Conclusions

Highly-conductive graphene was able to stimulate DIET to boost biomethane yield and production rate from ethanol. The addition of 1.0 g/L graphene resulted in an enhancement of 25.0% in biomethane yield and 19.5% in production rate. The degradation rate of ethanol was simultaneously enhanced. Electrogenic bacteria of *Geobacter* and *Pseudomonas* species along with archaea *Methanobacterium* and *Methanospirillum* might participate in DIET responsible for enhanced AD performance. Graphene-based DIET intrinsically sustained a much higher electron transfer flux than conventional hydrogen transfer. Reutilization of conductive materials should be considered to make DIET-based AD economically viable.

Acknowledgements

This collaborative Chinese Irish study was supported by the National key research and development program-China (2016YFE0117900), National Natural Science Foundation-China (51676171), Zhejiang Provincial Key Research and Development Program-China (2017C04001), and also funded by Science Foundation Ireland (SFI) through the Centre for Marine and

Renewable Energy (MaREI) under Grant No. 12/RC/2302. The work was also co-funded by Gas Networks Ireland (GNI) through the Gas Innovation Group, and by ERVIA.

References

[1] Adinaveen, T., Vijaya, J.J., Kennedy, L.J. 2016. Comparative Study of Electrical Conductivity on Activated Carbons Prepared from Various Cellulose Materials. *Arabian Journal for Science and Engineering*, **41**, 55-65.

[2] Ariunbaatar, J., Panico, A., Esposito, G., Pirozzi, F., Lens, P.N.L. 2014. Pretreatment methods to enhance anaerobic digestion of organic solid waste. *Applied Energy*, **123**, 143-156.

[3] Baena, S., Fardeau, M.L., Labat, M., Ollivier, B., Thomas, P., Garcia, J.L., Patel, B.K.C. 1998. Aminobacterium colombiensegen. nov. sp. nov., an Amino Acid-degrading Anaerobe Isolated from Anaerobic Sludge. *Anaerobe*, **4**, 241-250.

[4] Carballa, M., Duran, C., Hospido, A. 2011. Should We Pretreat Solid Waste Prior to Anaerobic Digestion? An Assessment of Its Environmental Cost. *Environmental Science & Technology*, **45**, 10306-10314.

[5] Catherine, M.S., Joey, M., Farid, A., Alex, L., Rigoberto, C.A., Debora, F.R. 2012. Graphene nanocomposite for biomedical applications: fabrication, antimicrobial and cytotoxic investigations. *Nanotechnology*, **23**, 395101.

[6] Chen, G., Zhao, L., Qi, Y. 2015. Enhancing the productivity of microalgae cultivated in wastewater toward biofuel production: A critical review. *Applied Energy*, **137**, 282-291.

[7] Cheng, J., Sun, J., Huang, Y., Feng, J., Zhou, J., Cen, K. 2013. Dynamic microstructures

and fractal characterization of cell wall disruption for microwave irradiation-assisted lipid extraction from wet microalgae. *Bioresource Technology*, **150**, 67-72.

[8] Cheng, Q., Call, D.F. 2016. Hardwiring microbes via direct interspecies electron transfer: mechanisms and applications. *Environmental Science: Processes & Impacts*, **18**, 968-980.

[9] DeSantis, T.Z., Hugenholtz, P., Larsen, N., Rojas, M., Brodie, E.L., Keller, K., Huber, T., Dalevi, D., Hu, P., Andersen, G.L. 2006. Greengenes, a Chimera-Checked 16S rRNA Gene Database and Workbench Compatible with ARB. *Applied and Environmental Microbiology*, **72**, 5069-5072.

[10] ElMekawy, A., Hegab, H.M., Losic, D., Saint, C.P., Pant, D. 2016. Applications of graphene in microbial fuel cells: The gap between promise and reality. *Renewable and Sustainable Energy Reviews*.

[11] Freguia, S., Teh, E.H., Boon, N., Leung, K.M., Keller, J., Rabaey, K. 2010. Microbial fuel cells operating on mixed fatty acids. *Bioresource Technology*, **101**, 1233-1238.

[12] Kato, S., Hashimoto, K., Watanabe, K. 2012. Methanogenesis facilitated by electric syntrophy via (semi)conductive iron-oxide minerals. *Environmental Microbiology*, **14**, 1646-1654.

[13] Kusiak, A., Wei, X. 2012. Optimization of the activated sludge process. *Journal of Energy Engineering*, **139**, 12-17.

[14] Lee, J.Y., Lee, S.H., Park, H.D. 2016. Enrichment of specific electro-active microorganisms and enhancement of methane production by adding granular activated carbon in anaerobic reactors. *Bioresour Technol*, **205**, 205-12.

[15] Lee, Y.-J., Romanek, C.S., Wiegel, J. 2007. Clostridium aciditolerans sp. nov., an

acid-tolerant spore-forming anaerobic bacterium from constructed wetland sediment. *International Journal of Systematic and Evolutionary Microbiology*, **57**, 311-315.

[16] Li, L.L., Tong, Z.H., Fang, C.Y., Chu, J., Yu, H.Q. 2015. Response of anaerobic granular sludge to single-wall carbon nanotube exposure. *Water Research*, **70**, 1-8.

[17] Lin, R., Cheng, J., Ding, L., Song, W., Liu, M., Zhou, J., Cen, K. 2016. Enhanced dark hydrogen fermentation by addition of ferric oxide nanoparticles using Enterobacter aerogenes. *Bioresource Technology*, **207**, 213-219.

[18] Liu, F.H., Rotaru, A.E., Shrestha, P.M., Malvankar, N.S., Nevin, K.P., Lovley, D.R. 2012. Promoting direct interspecies electron transfer with activated carbon. *Energy & Environmental Science*, **5**, 8982-8989.

[19] Liu, S., Zeng, T.H., Hofmann, M., Burcombe, E., Wei, J., Jiang, R., Kong, J., Chen, Y. 2011. Antibacterial Activity of Graphite, Graphite Oxide, Graphene Oxide, and Reduced Graphene Oxide: Membrane and Oxidative Stress. *ACS Nano*, **5**, 6971-6980.

[20] Lovley, D.R. 2006. Bug juice: harvesting electricity with microorganisms. *Nat Rev Microbiol*, **4**, 497-508.

[21] Lovley, D.R. 2011. Live wires: direct extracellular electron exchange for bioenergy and the bioremediation of energy-related contamination. *Energy & Environmental Science*, **4**, 4896-4906.

[22] Lovley, D.R., Ueki, T., Zhang, T., Malvankar, N.S., Shrestha, P.M., Flanagan, K.A., Aklujkar, M., Butler, J.E., Giloteaux, L., Rotaru, A.E., Holmes, D.E., Franks, A.E., Orellana, R., Risso, C., Nevin, K.P. 2011. Geobacter: the microbe electric's physiology, ecology, and practical applications. *Adv Microb Physiol*, **59**, 1-100.

[23] Mao, X., Stenuit, B., Polasko, A., Alvarez-Cohen, L. 2015. Efficient Metabolic Exchange and Electron Transfer within a Syntrophic Trichloroethene-Degrading Coculture of Dehalococcoides mccartyi 195 and Syntrophomonas wolfei. *Applied and Environmental Microbiology*, **81**, 2015-2024.

[24] Morita, M., Malvankar, N.S., Franks, A.E., Summers, Z.M., Giloteaux, L., Rotaru, A.E., Rotaru, C., Lovley, D.R. 2011. Potential for Direct Interspecies Electron Transfer in Methanogenic Wastewater Digester Aggregates. *mBio*, **2**, e00159-11.

[25] Nguyen, H.N., Castro-Wallace, S.L., Rodrigues, D.F. 2017. Acute toxicity of graphene nanoplatelets on biological wastewater treatment process. *Environmental Science: Nano*, **4**, 160-169.

[26] Nigam, P.S., Singh, A. 2011. Production of liquid biofuels from renewable resources. *Progress in Energy and Combustion Science*, **37**, 52-68.

[27] Pasquini, L.M., Hashmi, S.M., Sommer, T.J., Elimelech, M., Zimmerman, J.B. 2012. Impact of surface functionalization on bacterial cytotoxicity of single-walled carbon nanotubes. *Environ. Sci. Technol.*, **46**, 6297.

[28] Perreault, F., Fonseca de Faria, A., Elimelech, M. 2015. Environmental applications of graphene-based nanomaterials. *Chem Soc Rev*, **44**, 5861-5896.

[29] Qu, Y., Ma, Q., Deng, J., Shen, W., Zhang, X., He, Z., Van Nostrand, J.D., Zhou, J., Zhou, J. 2015. Responses of microbial communities to single-walled carbon nanotubes in phenol wastewater treatment systems. *Environ Sci Technol*, **49**, 4627-35.

[30] Reguera, G., McCarthy, K.D., Mehta, T., Nicoll, J.S., Tuominen, M.T., Lovley, D.R. 2005. Extracellular electron transfer via microbial nanowires. *Nature*, **435**, 1098-101.

[31] Rotaru, A.E., Shrestha, P.M., Liu, F., Markovaite, B., Chen, S., Nevin, K.P., Lovley, D.R. 2014a. Direct Interspecies Electron Transfer between Geobacter metallireducens and Methanosarcina barkeri. *Applied and Environmental Microbiology*, **80**, 4599-4605.

[32] Rotaru, A.E., Shrestha, P.M., Liu, F.H., Shrestha, M., Shrestha, D., Embree, M., Zengler, K., Wardman, C., Nevin, K.P., Lovley, D.R. 2014b. A new model for electron flow during anaerobic digestion: direct interspecies electron transfer to Methanosaeta for the reduction of carbon dioxide to methane. *Energy & Environmental Science*, **7**, 408-415.

[33] Schink, B. 1997. Energetics of syntrophic cooperation in methanogenic degradation. *Microbiology and Molecular Biology Reviews*, **61**, 262-280.

[34] Shen, Y., Linville, J.L., Urgun-Demirtas, M., Schoene, R.P., Snyder, S.W. 2015. Producing pipeline-quality biomethane via anaerobic digestion of sludge amended with corn stover biochar with in-situ CO2 removal. *Applied Energy*, **158**, 300-309.

[35] Shrestha, P.M., Malvankar, N.S., Werner, J.J., Franks, A.E., Elena-Rotaru, A., Shrestha, M., Liu, F.H., Nevin, K.P., Angenent, L.T., Lovley, D.R. 2014. Correlation between microbial community and granule conductivity in anaerobic bioreactors for brewery wastewater treatment. *Bioresource Technology*, **174**, 306-310.

[36] Stams, A.J.M., Plugge, C.M. 2009. Electron transfer in syntrophic communities of anaerobic bacteria and archaea. *Nature Reviews Microbiology*, **7**, 568-577.

[37] Storck, T., Virdis, B., Batstone, D.J. 2016. Modelling extracellular limitations for mediated versus direct interspecies electron transfer. *The ISME journal*, **10**, 621-631.

[38] Summers, Z.M., Fogarty, H.E., Leang, C., Franks, A.E., Malvankar, N.S., Lovley, D.R. 2010. Direct Exchange of Electrons Within Aggregates of an Evolved Syntrophic

Coculture of Anaerobic Bacteria. *Science*, **330**, 1413-1415.

[39] Tian, T., Qiao, S., Li, X., Zhang, M., Zhou, J. 2017. Nano-graphene induced positive effects on methanogenesis in anaerobic digestion. *Bioresource Technology*, **224**, 41-47.

[40] Torrijos, M. 2016. State of Development of Biogas Production in Europe. *Procedia Environmental Sciences*, **35**, 881-889.

[41] Viggi, C.C., Rossetti, S., Fazi, S., Paiano, P., Majone, M., Aulenta, F. 2014. Magnetite Particles Triggering a Faster and More Robust Syntrophic Pathway of Methanogenic Propionate Degradation. *Environmental Science & Technology*, **48**, 7536-7543.

[42] Wei, X., Kusiak, A. 2012. Optimization of biogas production process in a wastewater treatment plant. *IIE Annual Conference. Proceedings*. Institute of Industrial and Systems Engineers (IISE). pp. 1.

[43] Xia, A., Jacob, A., Herrmann, C., Tabassum, M.R., Murphy, J.D. 2015. Production of hydrogen, ethanol and volatile fatty acids from the seaweed carbohydrate mannitol. *Bioresource Technology*, **193**, 488-497.

[44] Xia, A., Jacob, A., Tabassum, M.R., Herrmann, C., Murphy, J.D. 2016. Production of hydrogen, ethanol and volatile fatty acids through co-fermentation of macro- and micro-algae. *Bioresource Technology*, **205**, 118-125.

[45] Yamada, T., Sekiguchi, Y., Hanada, S., Imachi, H., Ohashi, A., Harada, H., Kamagata, Y. 2006. Anaerolinea thermolimosa sp. nov., Levilinea saccharolytica gen. nov., sp. nov. and Leptolinea tardivitalis gen. nov., sp. nov., novel filamentous anaerobes, and description of the new classes Anaerolineae classis nov. and Caldilineae classis nov. in the bacterial phylum Chloroflexi. *International Journal of Systematic and Evolutionary Microbiology*,

56, 1331-1340.

[46] Zhao, Z., Zhang, Y., Holmes, D.E., Dang, Y., Woodard, T.L., Nevin, K.P., Lovley, D.R. 2016a. Potential enhancement of direct interspecies electron transfer for syntrophic metabolism of propionate and butyrate with biochar in up-flow anaerobic sludge blanket reactors. *Bioresour Technol*, **209**, 148-56.

[47] Zhao, Z., Zhang, Y., Yu, Q., Dang, Y., Li, Y., Quan, X. 2016b. Communities stimulated with ethanol to perform direct interspecies electron transfer for syntrophic metabolism of propionate and butyrate. *Water Res*, **102**, 475-84.

[48] Zhao, Z.Q., Zhang, Y.B., Woodard, T.L., Nevin, K.P., Lovley, D.R. 2015. Enhancing syntrophic metabolism in up-flow anaerobic sludge blanket reactors with conductive carbon materials. *Bioresource Technology*, **191**, 140-145.

[49] Zhu, B., Xia, X., Xia, N., Zhang, S., Guo, X. 2014. Modification of fatty acids in membranes of bacteria: implication for an adaptive mechanism to the toxicity of carbon nanotubes. *Environ. Sci. Technol.*, **48**, 4086.

List of figures and tables:

Fig. 1 Effects of graphene and activated charcoal on biomethane yield and production rate from ethanol: (a) biomethane yield, (b) biomethane production rate.

Fig. 2 Effects of graphene and activated charcoal on ethanol and acetate conversion: (a) ethanol degradation kinetics, (b) ethanol degradation rate constant, (c) acetate degradation, and (d) overall electron recovery.

Fig. 3 Mechanisms for extracellular cell-to-cell electron transfer in anaerobic digestion: (a) mediated interspecies electron transfer, (b) direct interspecies electron transfer via graphene.

Table1 Effects of graphene and activated charcoal on biomethane production kinetics.

Table 2 Three step reactions and thermodynamics in bioconversion of ethanol to biomethane.

Table 3 Bacterial community structures at genus level with/without graphene addition after anaerobic digestion of ethanol. Genera with less than 1% abundances were classified into others.

Table 4 Archaeal community structures at genus level with/without graphene addition after anaerobic digestion of ethanol. Genera with less than 1% abundances were classified into others.

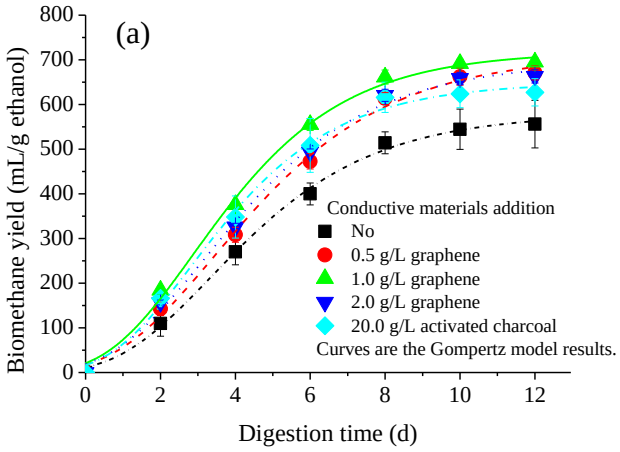

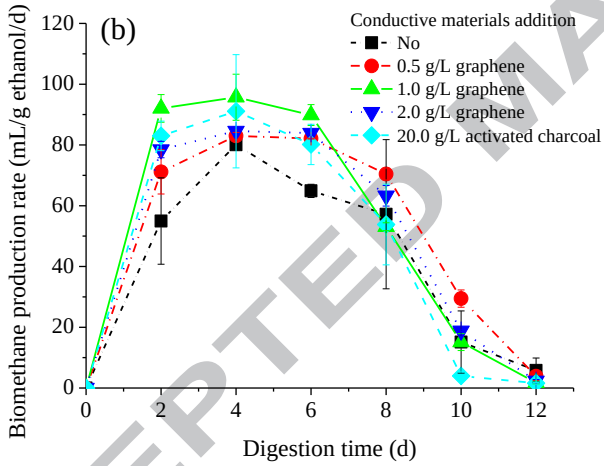

Fig. 1 Effects of graphene and activated charcoal on biomethane yield and production rate from ethanol: (a) biomethane yield, (b) biomethane production rate. Results are the means and standard deviations for duplicate experiments.

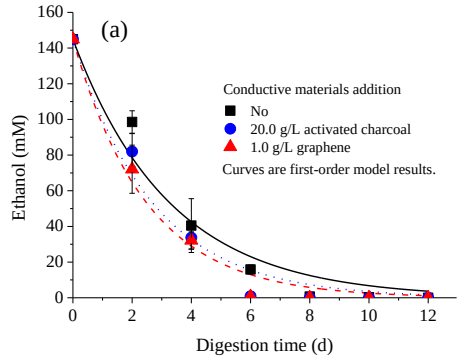

1

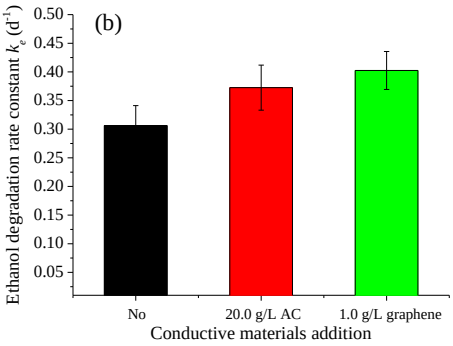

2

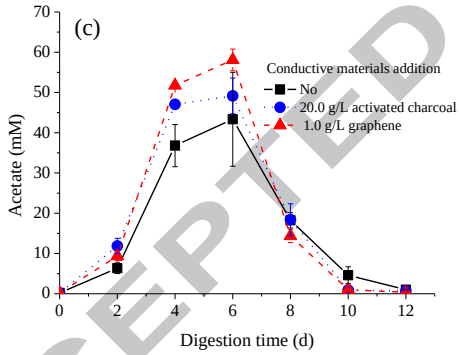

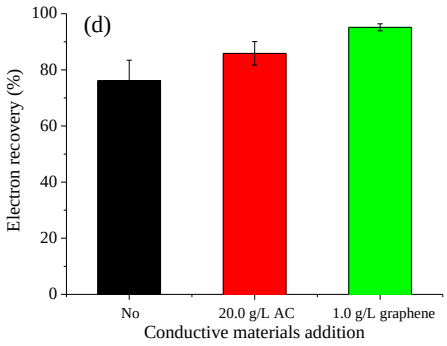

3

4 Fig. 2 Effects of graphene and activated charcoal on ethanol and acetate conversion: (a) ethanol
5 degradation kinetics, (b) ethanol degradation rate constant, (c) acetate degradation, and (d) overall
6 electron recovery. Results are the means and standard deviations for duplicate experiments.

1

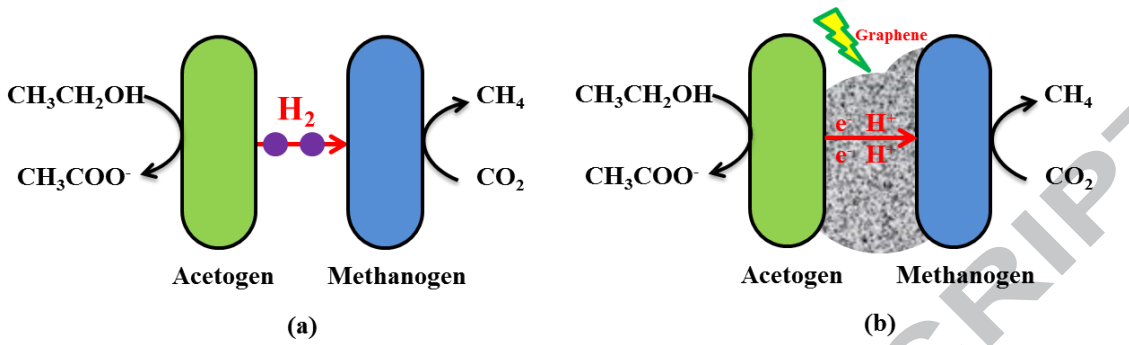

2

3 Fig. 3 Mechanisms for extracellular cell-to-cell electron transfer in anaerobic digestion: (a)

4 mediated interspecies electron transfer, (b) direct interspecies electron transfer via graphene.

5

Table1 Effects of graphene and activated charcoal on biomethane production kinetics.

Conductive materials concentration	Biomethane yield (mL/g)	Peak biomethane production rate (mL/g/d)	Kinetic model parameters				
			H_m (mL/g)	R_m (mL/g/d)	λ (d)	T_m (d)	R^2
No	556.1±53.3	80.1±0.2	579.7	86.9	0.89	3.34	0.9967
0.5 g/L graphene	670.9±16.0	83.0±1.1	711.2	99.1	0.81	3.45	0.9951
1.0 g/L graphene	695.0±9.1	95.7±7.6	718.4	116.2	0.60	2.87	0.9955
2.0 g/L graphene	662.9±14.7	84.6±1.3	695.7	102.8	0.70	3.19	0.9950
20.0 g/L activated charcoal	627.2±30.7	91.1±18.6	648.8	109.8	0.65	2.82	0.9939

Note: H_m, maximum methane yield potential; R_m, peak methane production rate; λ, lag-phase time; and T_m, peak time of methane fermentation.

Table 2 Three step reactions and thermodynamics in bioconversion of ethanol to biomethane.

Process	Reactions	$\Delta G_0'$[a] (kJ/mol)
1. Electron-producing acetogen	MIET: $CH_3CH_2OH + H_2O \rightarrow CH_3COO^- + H^+ + 2H_2$	9.68
	DIET: $CH_3CH_2OH + H_2O \rightarrow CH_3COO^- + 5H^+ + 4e^-$	-149.64
2. Electron-consuming methanogen	MIET: $2H_2 + 1/2CO_2 \rightarrow 1/2CH_4 + H_2O$	-65.35
	DIET: $4H^+ + 4e^- + 1/2CO_2 \rightarrow 1/2CH_4 + H_2O$	93.98
3. Acetate-consuming methanogen	$CH_3COO^- + H^+ \rightarrow CH_4 + CO_2$	-35.91
Overall	$CH_3CH_2OH \rightarrow 3/2CH_4 + 1/2CO_2$	-91.58

[a] $\Delta G_0'$ is the free energy change of reaction under standard conditions at pH 7. Negative value indicates the reaction is thermodynamically favorable and proceeds spontaneously.

12 Table 3 Bacterial community structures at genus level with/without graphene addition after anaerobic digestion of ethanol. Genera with less than 1% abundances

13 were classified into others.

	Relative abundance in different anaerobic digestates (%)		
Genera	Inoculum	Digestate without graphene	Digestate with 1.0 g/L graphene
Geobacter	0.29	8.43	9.94
Pseudomonas	0.43	1.91	6.85
Levilinea	7.64	11.59	6.2
Clostridium	10.09	8.57	5.15
Thermovirga	3.34	2.71	2.98
Victivallis	0.38	2.89	2.73
Aminobacterium	3.98	2.14	2.24
Longilinea	0.85	2.71	2.22
Desulfovibrio	0.05	2.27	1.96
Synergistes	3.09	1.97	1.72
Smithella	2.86	2.03	1.45
Syntrophomonas	1.4	2.13	1.27
Meniscus	1.86	1.69	1.24
Bellilinea	1.27	1.54	0.9
Others	42.92	34.04	39.39
unclassified	19.55	13.38	13.76

14

15

16 Table 4 Archaeal community structures at genus level with/without graphene addition after anaerobic digestion of ethanol. Genera with less than 1% abundances

17 were classified into others.

	Relative abundance in different anaerobic digestates (%)		
Genera	Inoculum	Digestate without graphene	Digestate with 1.0 g/L graphene
Methanosaeta	86.08	50.14	39.75
Methanobacterium	2.68	24.02	34.87
Methanolinea	6.44	20.19	9.84
Methanospirillum	1.14	2.15	7.76
unclassified	2.27	2.07	4.66
Others	1.39	1.43	3.12

18

19

Graphical abstract

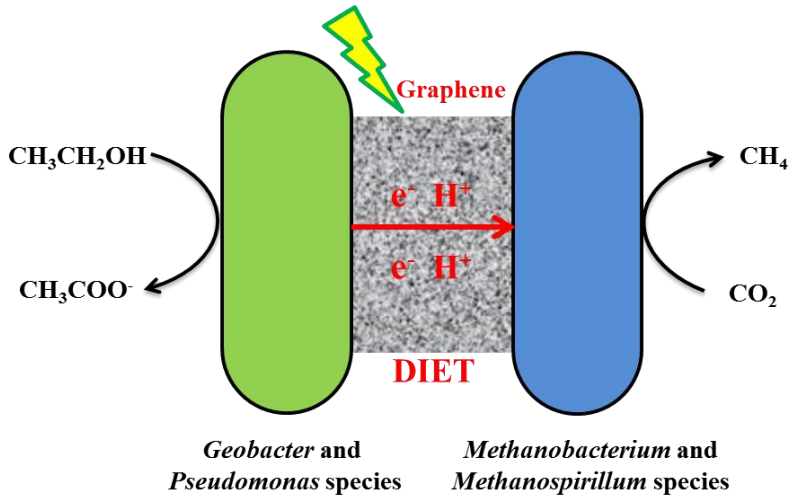

Graphene-based DIET in anaerobic digestion

- Graphene enhanced methane yield (+25%) and production rate (+20%) in AD of ethanol.
- Microbial structures of electro-active bacteria and archaea were revealed after AD.
- Direct interspecies electron transfer (DIET) via graphene was established in AD.
- DIET sustained much higher electron transfer flux than hydrogen transfer.